

Influence of reactive diluent composition on properties and bio-based content of itaconic acid-based additive manufacturing materials

Original

Influence of reactive diluent composition on properties and bio-based content of itaconic acid-based additive manufacturing materials / Papadopoulos, Lazaros; Pezzana, Lorenzo; Malitowski, Natalia; Sangermano, Marco; Bikiaris, Dimitrios N.; Robert, Tobias. - In: DISCOVER APPLIED SCIENCES. - ISSN 3004-9261. - ELETTRONICO. - 6:6(2024). [10.1007/s42452-024-05926-x]

Availability:

This version is available at: 11583/2988983 since: 2024-05-24T16:06:01Z

Publisher:

springer

Published

DOI:10.1007/s42452-024-05926-x

Terms of use:

This article is made available under terms and conditions as specified in the corresponding bibliographic description in the repository

Publisher copyright

(Article begins on next page)


Research

Influence of reactive diluent composition on properties and bio-based content of itaconic acid-based additive manufacturing materials

Lazaros Papadopoulos¹  · Lorenzo Pezzana²  · Natalia Malitowski³ · Marco Sangermano²  ·
Dimitrios N. Bikiaris¹  · Tobias Robert³ 

Received: 14 October 2023 / Accepted: 29 April 2024

Published online: 23 May 2024

© The Author(s) 2024 

Abstract

Among the additive manufacturing techniques, UV-curing processes are of special interest, as they allow for the fabrication of thermosetting materials with high resolutions and optical clarity. Traditionally, these processes require the use of formulations, consisting of polyester or polyurethane oligomers, combined with photoinitiators and reactive diluents. The latter are usually vinyl monomers such as acrylates or acrylamides, used to reduce the viscosity of the formulation and render it processable by additive manufacturing machines. In this work, we investigate whether a combination of diluents can be used to tune the thermomechanical properties of the printed materials, and if it can be exploited to increase their overall bio-based content without compromising their performance. To do so, a series of itaconic acid-based polyesters with different chemical structures (aliphatic–aromatic) were synthesized and formulated with reactive diluents acryloyl morpholine (ACMO) and isobornyl acrylate (IBOA). The physicochemical properties of the prepared formulations, together with their reactivity towards UV-light were assessed via photo differential scanning calorimetry (photo-DSC) and photo-rheology measurements. The same formulations were then used to fabricate test specimen via digital light processing (DLP) 3D printing, which were characterized on their thermomechanical properties by means of dynamic mechanical analysis (DMA) and thermogravimetric analysis (TGA) measurements. The glass transition temperature of the printed samples reached a maximum of 98 °C, while the diluent ratio could be used to manipulate the T_g in a linear trend. All materials of this study exhibited $T_{d,5\%}$ above 250 °C, suggesting good thermal stability. These results show that materials with a very high bio-based content (up to 85%) and very promising thermomechanical properties could be obtained by employing a diluent mixture during the formulation phase.

Keywords Additive manufacturing · Bio-based materials · Itaconic acid-based polyesters · Reactive diluents

Supplementary Information The online version contains supplementary material available at <https://doi.org/10.1007/s42452-024-05926-x>.

✉ Dimitrios N. Bikiaris, dbic@chem.auth.gr; ✉ Tobias Robert, tobias.robert@wki.fraunhofer.de | ¹Laboratory of Polymer Chemistry and Technology, Department of Chemistry, Aristotle University of Thessaloniki, 541 24 Thessaloniki, Greece. ²Dipartimento Scienza Applicata e Tecnologia, Politecnico di Torino, C.So Duca degli Abruzzi 24, 10129 Turin, Italy. ³Fraunhofer Institute for Wood Research - Wilhelm-Klauditz-Institut WKI, Riedenkamp 3, 38108 Braunschweig, Germany.



1 Introduction

Since its invention in the early 1980s, additive manufacturing (AM), also known as 3D-printing, has come a long way from a niche technique for prototyping applications to a well-established innovative fabrication technique [1]. In comparison with traditional formative methods, AM offers significant advantages, such as high individualization degree, waste reduction, fabrication of highly complex structures and low-cost AM-machines [2]. Depending on the envisaged application, different materials can be employed by AM-processes with polymers being one of the most important categories among them [3]. Within the different polymeric AM-methods, photo-curing processes have attracted attention, as they allow the shaping of thermosetting polymers into 3D-printed objects that exhibit very high levels of details. Furthermore, it also allows for transparent parts, which are not accessible by other thermo-plastic AM-processes. Three different techniques are currently applied in photo-curing processes. Stereolithography (SLA) and digital light processing (DLP) are using a resin vat in which the object is cured layer-wise by either a laser or a projector [4–8]. In the case of multi-jet modelling (MJM) on the other hand, the resin is deposited layer-wise by ink-jet nozzles and each layer is directly photo-cured. Typical polymer types that are employed in these processes are epoxide-based polymers for cationic curing systems and polyester and polyurethane acrylates for radical curing systems [9]. In addition to the latter, unsaturated polyesters derived from itaconic acid have recently been shown to be suitable polymers for additive manufacturing [10–12]. As our contribution to this field of materials, we recently published the application of a family of bio-based polyester itaconates [13, 14]. Moreover, the influence of secondary acids on the performance of the resins, as well as the cured materials was intensively studied. [15]

In addition to photo-curing polymers, formulations for additive manufacturing also contain significant amounts of reactive diluents. Despite the development of “specialty” printers that can process formulations of higher viscosities, conventional AM-machines require a maximum viscosity of 5 Pa·s to function [16]. While the addition of diluents in high contents can sometimes sacrifice the original mechanical properties of the oligomers [17], by careful selection the properties of the cured parts can be significantly improved. This is a result of both the structure of the diluent, as well as the fact that formulations with reduced viscosity allow for higher mobility of the system and in turn for a higher crosslinking density of the cured materials [17, 18]. Typical examples of reactive diluents employed are (meth) acrylates or other highly reactive vinyl monomers. Nevertheless, the introduction of diluents into the formulation comes with certain drawbacks. For example, some of these substances have been identified as harmful for human health [18–20], like *N*-vinyl caprolactam that has been studied as a diluent for stimuli-sensitive materials [21]. Furthermore, the majority of the monomers that are typically utilized as diluents are derived from fossil resources, contributing to greenhouse gas emissions and to the depletion of non-renewable resources [13]. So, in an effort to render AM more sustainable, greener substitutes for existing reactive diluents must be explored. In this respect, Su et al. prepared a diluent based on cardanol, a bio-based monomer with an aromatic structure, that exhibited low viscosity and good miscibility with acrylated epoxidized soybean oil (AESO), while also reducing the volume shrinkage of the crosslinked materials [22]. Wei et al. modified isosorbide, another bio-based monomer with a cyclic structure, to create isosorbide dimethacrylate, a diluent of adequate solubility that increased the glass transition and E' modulus of the crosslinked materials [23]. As a contribution from our labs, we studied the potential of itaconic acid-based monomers as diluents for acrylate-free AM-materials. [14]

Nevertheless, before the complete substitution of fossil-based diluents, more steps need to be taken, as the alternatives that are available presently come at a higher cost and often with reduced reactivity [24]. Until these issues are solved, other pathways to improve the sustainability of polyester-itaconates must be explored. As one possibility, we recently increased the overall bio-based content by reduction of the concentration of the reactive diluent concentration acryloyl morpholine (ACMO). We were able to show that even at concentrations of less than 30% of diluent, the printing performance as well as properties of itaconic acid-based AM-materials could compete with formulation with higher concentrations [25]. Another potential strategy could be the combination of petrochemical with bio-based diluents. This way, the processability of the formulations would be retained, the overall bio-based content could be improved and the thermomechanical properties of the printed materials could be manipulated by the utilized ratio of diluents. Interestingly enough, this route has not been explored so far in the field of itaconic acid-based unsaturated polyester resins. Therefore, in this study we employed two reactive diluents, the fossil-based ACMO and isobornyl acrylate (IBOA), which is 75% bio-based [26]. Those diluents were combined with unsaturated polyesters of high bio-based content, based on itaconic acid. Different ratios between the two diluents were examined. The physicochemical properties of the produced formulations were characterized and their reactivity towards UV light and their processability on a DLP-machine were also assessed.

2 Materials and methods

2.1 Materials

Itaconic acid (IA, 99%), succinic acid (SA, 99%), sebacic acid (SebA, 99%), isophthalic acid (IsA, 99%), phthalic anhydride (PhA, 99%), and 1,12-dodecanediol (DoDO, 98%) were purchased from Merck, Darmstadt, Germany. 1,3-Propanediol (PDO, 99.7%) was kindly provided by DuPont Tate & Lyle Bio Products, Loudon, NH, USA. FASCAT 4101 catalyst was kindly provided by PMC Group, Mount Laurel, NJ, USA. Acryloyl morpholine (ACMO, 99%) and isobornyl acrylate (IBOA, 99%) were purchased from Rahn GmbH, Frankfurt, Germany. TPO (Diphenyl(2,4,6-trimethylbenzoyl)phosphine oxide) was purchased from IGM Resins. All reagents were used without further purification.

2.2 Resin synthesis

The synthesis of the unsaturated polyesters has been described in length in our previous work [15]. In brief, the resins were prepared via a direct esterification reaction, at 180 °C, with a diacid to diol ratio of 1:1.45. They were obtained without further purification, as transparent viscous, slightly yellow to light brown liquids. The description of their composition is given in Table 1.

2.3 Formulation preparation

The preparation of the formulations described herein was done as follows: A ratio of polyester/reactive diluent/TPO of 0.5/0.47/0.03 was utilized, regardless of the components. For example, for the preparation of 50 g of Form-SebA-A 25 g of PE-SebA-50, 23.5 g of ACMO and 1.5 g of TPO were introduced to a lid-closing metal can, to prohibit light exposure. The mixture was left under stirring overnight until homogenization. These formulations were then used for all described characterizations and for AM experiments. The composition of all formulations can be found in Table 3. All are abbreviated as follows: Form for formulation, followed by the name of the polyester used and then the type of reactive diluent (A for ACMO, I for IBOA).

2.4 Measurements

Viscosity measurements were performed on a Malvern Kinexus lab+ (Malvern Panalytical Ltd, Malvern, UK) equipped with cone-plate geometry (CP 4°, 40 mm). Measurements were made with a rotation speed of 100 s⁻¹ for 10 s. Five measurements were made for each sample, and the average value was calculated.

Photo-differential scanning calorimetry (Photo-DSC) measurements were conducted on a DSC3⁺ (Mettler-Toledo, Greifensee, Switzerland) equipped with a Lightningcure LC8 UV spotlight source (Hamamatsu Photonics, Hamamatsu, Japan) at 70% of its maximum intensity. This corresponds to a total irradiance flux density (light density) of 175 mW/cm² provided on the surface of the sample. The lamp used is a mercury-xenon lamp with a broad irradiation spectrum with the highest intensity at 365 nm. To get the integration of the heat of reaction, two runs were carried out with a short break between the runs to let the resin cool down. The second run was made once the material was fully cured, and the baseline was stable. Then, the second curve was subtracted from the first to obtain the curve related to the curing only.

Table 1 Composition and bio-based content of the polyesters utilized in this study

Sample	IA (eq)	Secondary acid (eq)	PDO (eq)	DoDO (eq)	Bio-based content ¹ (wt%)
PE-SebA-50	0.5	0.5 SebA	1.45	–	100
PE-IsA-50		0.5 IsA	1.45	–	68
PE-SA-50		0.5 SA	1.45	–	100
PE-PhA-50		0.5 PhA	1.45	–	70
PE-IsA-DoDO-50		0.5 IsA	0.725	0.725	76

¹% of mass of renewable monomers used for the synthesis of each resin

Each run is conducted as follows: 30 s at the set temperature of 25 °C, at atmospheric pressure under nitrogen without the lamp; then, the lamp is turned on for 4.5 min. The break between the runs lasts 30 s.

Photo-rheology data were collected by means of Anton Paar 302MC rheometer (Physica MCR 302, Graz, Styria). The rheometer was set with a plate-plate geometry, the outside diameter of the metal disk was 25 mm and a glass disk was used as bottom support in order to guarantee the irradiation of the sample. The distance between the two disks was set at 200 µm and the experiments were carried out at room temperature. The visible-light was provided by optic fiber to directly irradiate the sample. A Hamamatsu LIGHTINGCURE LC8 was used as visible-source with a light intensity of about 40 mW/cm² provided on the surface of the sample. The lamp was centered at 405 nm, to match the wavelength used during the 3D printing process. The lamp was turned on after 60 s of stabilization and the measurements were performed in oscillatory condition at frequency of 1 Hz, with strain 1% and in isothermal condition at room temperature. The study of the light intensity effect was conducted varying the UV-intensity according to Figure S1. The UV intensity was measured by ACCU-CAL™ 160 radiometer, positioned directly on top of the glass substrate of the rheometer.

Additive manufacturing experiments were conducted on a Phrozen Sonic 4K DLP printer equipped with a 50 W UV LED array (405 nm). The samples were cured with a layer thickness of 20 µm and an exposure time of 10 s per layer for formulations prepared from PE-IsA-50 and PE-IsA-DoDO-50. The rest of the formulations were cured with a curing time of 3 s per layer. Approximately forty grams of formulation were used to print five rectangle specimens at once, suitable for DMA measurements. After the process, samples were removed from the printer and post-cured in a post-curing light oven (Wanhao Boxman-1) for 30 min. The samples were turned after 15 min to ensure even curing of the specimens.

Dynamic mechanical analysis (DMA) was carried out on a Tritec 2000 DMA (Triton Technology, Loughborough, UK) in single cantilever bending mode. Measurements were performed on the rectangle bars (25 × 10 × 4 mm) which were prepared with additive manufacturing. Samples were studied under nitrogen in a temperature range of 0–150 °C (2 K min⁻¹, 1 Hz, maximum displacement 0.01 mm). The exact dimensions of specimens were determined before each experiment, and five test bars were measured for each sample. The crosslinking density of the crosslinked materials was evaluated according to the kinetic theory of rubber elasticity [27]:

$$\nu = \frac{E'}{3RT}$$

where E' is the storage modulus in the rubbery plateau region at $T = T_g + 30$ °C, R is the gas constant, and T is the absolute temperature in K . The glass transition of the printed materials is calculated as the peak of the $\tan \delta$ curves.

Thermogravimetric analysis (TGA) of cured resins was performed on a TGA/DSC 1 (Mettler-Toledo, Greifensee, Switzerland) under nitrogen (35 mL min⁻¹). Samples of ca. 10 mg were heated from 25 to 700 °C with a heating rate of 10 K min⁻¹.

Contact angle measurements were performed by means of a Drop Shape Analyzer, DSA100, Krüss (Germany), equipped with a video camera. The test was done measuring the contact angle of a water droplet on a free surface in a static mode. The reported results are an average of at least 5 water droplets.

3 Results and discussion

3.1 Formulation preparation

The main objective of the study presented herein is an in-depth investigation of the step-wise replacement of the petrochemical reactive diluent ACMO with the bio-based monomer IBOA in bio-based additive manufacturing formulations (Fig. 1). This was done to increase the overall bio-based content of these materials, and to manipulate their properties

Fig. 1 Chemical structure of reactive diluents ACMO and IBOA

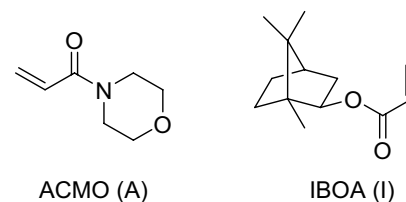
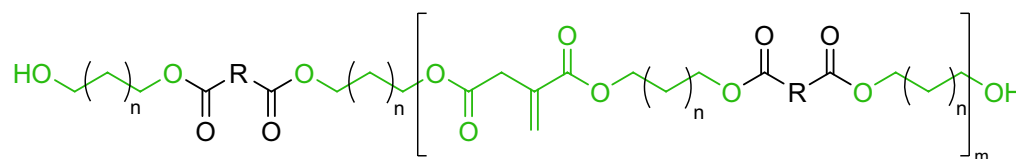


Table 2 Summary of the properties of the UPRs (uncured) utilized in this study

Sample	M_n (g/mol)	M_w (g/mol)	\bar{D}	T_g (°C)
PE-SebA-50	980	1980	2.04	< - 50 °C
PE-IsA-50	1290	2340	1.8	- 28.3 °C
PE-SA-50	920	1620	1.75	< - 50 °C
PE-PhA-50	910	1590	1.73	- 32.6 °C
PE-IsA-DoDO-50	1790	3350	1.87	< - 50 °C



secondary acid:

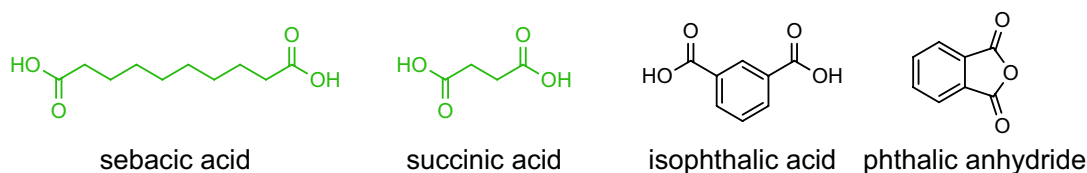


Fig. 2 Chemical structure of the polyesters of this study, bio-based monomers are shown in green

via the utilized ratio of diluents. As oligomeric component in these formulations, unsaturated polyester resins (UPRs) derived from bio-based itaconic acid are being used. These resins have been synthesized in our labs and were previously characterized [15]. Their properties are summarized in Table 2, and their structure is given in Fig. 2.

I BOA was selected as bio-based reactive diluent, as it is commercially available, partially bio-based (75%) and its cyclic structure can be beneficial for the mechanical properties of the crosslinked materials [26]. However, preliminary experiments showed that the selected group of resins was not entirely miscible with IBOA. Polyesters containing aliphatic secondary acids were miscible with IBOA and could form homogenous formulations, but those containing aromatic secondary acids were immiscible, resulting in phase separation of diluent and polyester resin.

These results were not expected, as in our previous work [15, [25] the same polyesters were found to be completely miscible with ACMO, another commercially available diluent derived from non-renewable feedstock. Even though both possess cyclic structures (Fig. 1) the more polar nature of the morpholine ring in ACMO compared with rather nonpolar bicyclic structure of IBOA seems to have quite a significant impact on the compatibility, especially with polyesters with aromatic building blocks, who did not form homogenous mixtures with IBOA in most cases. To overcome this impediment, we decided to utilize IBOA in combination with ACMO. For this, we herein prepared formulations of the polyesters in question, containing a 1:1 mix of ACMO and IBOA for the diluent part. All resins were soluble in the mixture of diluents, yielding homogenous formulations that were characterized on their reactivity towards UV-light induced radical crosslinking. Results were compared to the respective formulations that contained only ACMO as the reactive diluent. The obtained values are presented in Table 3.

The introduction of the mixture of diluents did not influence the viscosity of the formulations, as values were very similar to those of the formulations that only contained ACMO. On the other hand, photo-DSC (Figure S2) studies revealed that the maximum of the rate of polymerization (RoP_{max}) was lower for the formulations with mixture of diluents, because of lower reactivity of IBOA compared to ACMO. However, a slightly lower polymerization rate can be beneficial, allowing for an increased C=C double bond conversion, as observed in our previous study [25]. Indeed, these formulations exhibited similar or higher conversions compared to their ACMO analogues.

These results show that a partial substitution of ACMO with IBOA was possible, without compromising the reactivity or the processability of the formulations. Knowing that the complete replacement is not feasible when aromatic polyesters were used, the next question was to what extent can we substitute ACMO with IBOA while retaining a processable

Table 3 Summary of the properties of the prepared formulations

Formulation	Resin (50%)	Reactive diluent (wt%)	Viscosity @ 20 °C (Pa·s)	Bio-based content ¹	DBD ² (mmol/g)	RoP ³ (s ⁻¹ ·10 ³)	C ⁴ (%)
Form-SebA A	PE-SebA-50	47% ACMO	0.15	50	4.38	83.2	89.3
Form-IsA A	PE-IsA-50		0.72	34	4.43	72.7	77.7
Form-SA A	PE-SA-50		0.24	50	4.58	65.9	77.7
Form-PhA A	PE-PhA-50		0.49	35	4.43	62.2	75.1
Form-SebA A:I_1:1	PE-SebA-50	23.5% ACMO-23.5% IBOA	0.16	67.6	3.84	61	90
Form-IsA A:I_1:1	PE-IsA-50		0.61	51.6	3.89	77.8	76.9
Form-SA A:I_1:1	PE-SA-50		0.22	67.6	4.04	69.2	85.1
Form-PhA A:I_1:1	PE-PhA-50		0.47	52.6	3.89	62.6	80.4
Form-SebA I	PE-SebA-50	47% IBOA	0.17	85.2	3.3	51.3	95.1
Form-SA I	PE-SA-50		0.25	85.2	3.5	43.4	71
Form-IsA-DoDO A	PE-IsA-DoDO-50	47% ACMO	0.42	38	4.13	89.6	84.1
Form-IsA-DoDO A:I_3:1		35.25% ACMO-11.75% IBOA	0.41	46.8	3.86	71.4	82.9
Form-IsA-DoDO A:I_1:1		23.5% ACMO-23.5% IBOA	0.42	55.6	3.59	68.7	83.1
Form-IsA-DoDO A:I_1:3		11.75% ACMO-35.25% IBOA	0.37	64.4	3.32	60.2	85.1
Form-IsA-DoDO I		47% IBOA	0.43	73.3	3.06	48.7	86.3
Form-IsA A	PE-IsA-50	47% ACMO	0.72	34	4.43	72.7	77.7
Form-IsA A:I_1:3		35.25% ACMO-11.75% IBOA	1.57	42.8	4.16	72	74.8
Form-IsA A:I_1:1		23.5% ACMO-23.5% IBOA	0.61	51.6	3.89	77.8	76.9
Form-IsA A:I_1:3		11.75% ACMO-35.25% IBOA	0.57	60.4	3.62	42.4	69.4

¹% of mass of renewable monomers used for the preparation of each formulation; ²: Double Bond Density, calculated as the mmol of C=C double bonds per g of formulation; ³: Rate of Polymerization; ⁴: Conversion of C=C double bonds, calculated by photo-DSC

formulation. In addition, it was of interest how the introduction of IBOA would influence the properties of the materials fabricated from these formulations. In order to investigate this, we selected two aromatic polyesters of similar structure, but with different composition of the diols, one with PDO as sole diol component (PE-IsA-50) and another with a 1:1 ratio of PDO and DoDO (PE-IsA-DoDO-50). With these both resins, a total of nine formulations was prepared, with neat ACMO, 3:1 ACMO:IBOA (A:I_3:1), 1:1 ACMO:IBOA (A:I_1:1) and 1:3 ACMO:IBOA (A:I_1:3) ratio. A neat IBOA formulation was created only for PE-IsA-DoDO-50, as PE-IsA-50 did not form a homogenous mixture. All created formulations and their composition are listed in Table 3.

Formulations derived from the same polyester resin exhibited very similar viscosities, regardless of the diluent compositions used. Formulations of PE-IsA-50 presented higher viscosity overall, as PE-IsA-50 is more viscous than PE-IsA-DoDO-50, but in all cases, viscosity of all formulations is well below 2 Pa·s, which makes them easily processable on standard AM-machines.

3.2 Photo-DSC

The reactivity of all formulations was analyzed by means of photo-DSC. Here a significant difference in the curing behavior was observed when ACMO was replaced by IBOA. Introduction of the latter to formulations of PE-IsA-DoDO-50 resulted in a linear decrease of the RoP_{max} , starting from $90 \text{ s}^{-1} \cdot 10^3$ for neat ACMO and limited to $49 \text{ s}^{-1} \cdot 10^3$ for neat IBOA (Fig. 4). Despite the slower rate, the overall conversion of the C=C double bonds was not affected, as for all formulations values between 83 and 86% were recorded (Fig. 3). Those values were calculated under the assumption that acrylate and itaconate double bonds have similar kinetics during homo- and copolymerization, utilizing the theoretical maximum enthalpy liberated by a mole of ACMO (acrylamide was used as reference: $\Delta H_{acrylamide \text{ theo}}: 82.64 \text{ kJ/mol}$) [28, 29] and a mole of substituted itaconate (dimethyl itaconate was used as reference: $\Delta H_{DMI \text{ theo}}: 60.67 \text{ kJ/mol}$) [30]. On the other hand, formulations of PE-IsA-50 presented a very similar behavior concerning the polymerization rate and the overall C=C conversion, until the 1:1 ACMO:IBOA loading. Moving to a 1:3 ACMO:IBOA ratio changed the behavior of the formulation significantly, reducing the polymerization rate and the conversion by 40% and 10% respectively. Also, when compared with the respective formulation from PE-IsA-DoDO-50, the rate is approximately 30% lower and the C=C conversion is

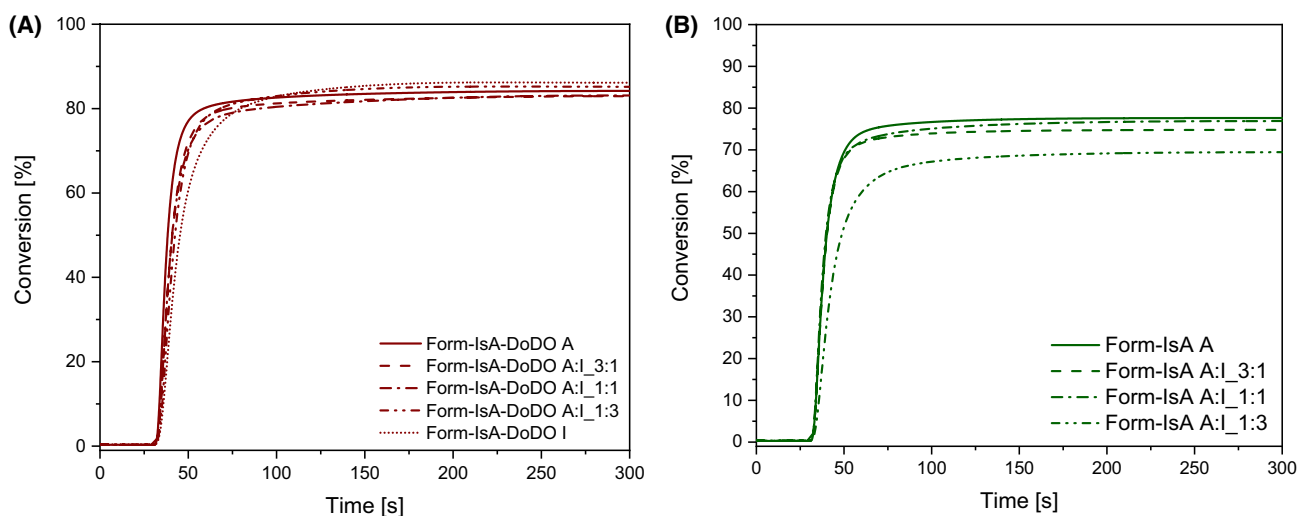


Fig. 3 C=C double bond conversion of the formulations based on (A) PE-Isa-DoDO-50 and (B) PE-IsA-50

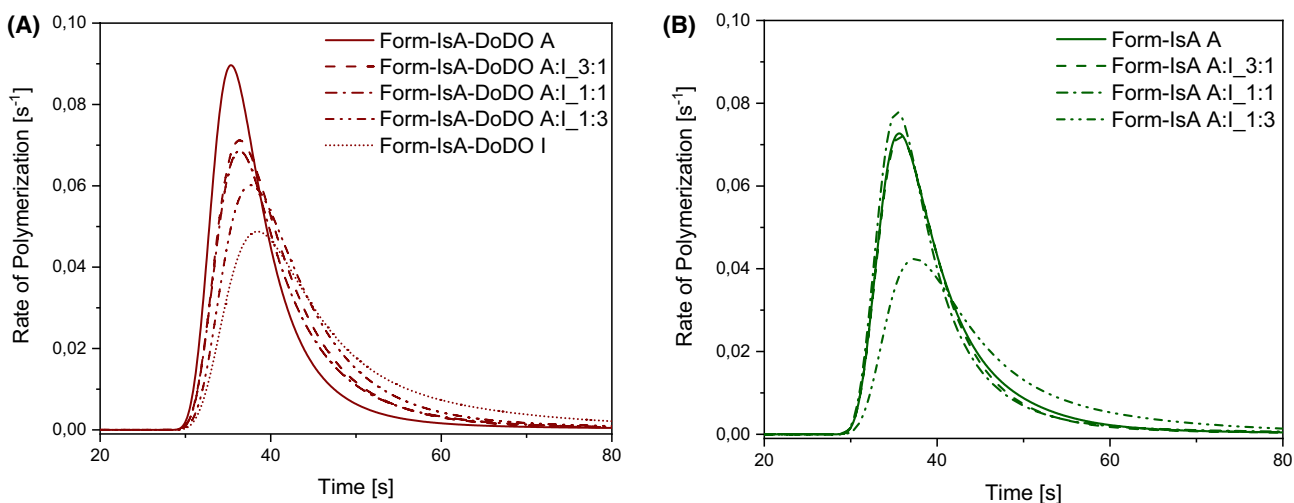


Fig. 4 Polymerization rate of the formulations based on (A) PE-Isa-DoDO-50 and (B) PE-IsA-50. The lamp is started after 30 s

reduced by 16%. It became clear, that for this group of formulations (based on PE-IsA-50), a different behavior is to be expected with the addition of IBOA to the mixture, potentially because of the more rigid nature of this polyester due to the higher aromatic content. Unfortunately, the preparation of a formulation where IBOA was the only diluent was again not possible, which makes a comparison to the other materials difficult (Fig. 4).

3.3 Photo rheology

To further assess the reactivity of the formulations, photo rheology experiments were conducted. The results are presented in Fig. 5. Similar to the results obtained from the photo-DSC measurements, the reactivity of the formulations decreases with increasing amounts of IBOA. This behavior was displayed as a longer induction time until the crosslinking-induced viscosity increase, caused by the UV-light irradiation of the formulation. However, the reactivity of all samples remains high, as the plateau is reached in a matter of seconds from the beginning of the irradiation for all formulations. This suggests the possibility of employing AM to process our formulations, as the curing time is comparable to standard layer irradiation times that are used in DLP 3D printing. Furthermore, the effect of light intensity on the curing of the formulations derived from PE-IsA-DoDO-50 was investigated. Results are shown in Fig. 6 and Figure S2. Decreasing the light intensity led to higher induction times. However, the slope of the increase of the storage modulus remained almost unchanged regardless of the light intensity, suggesting a

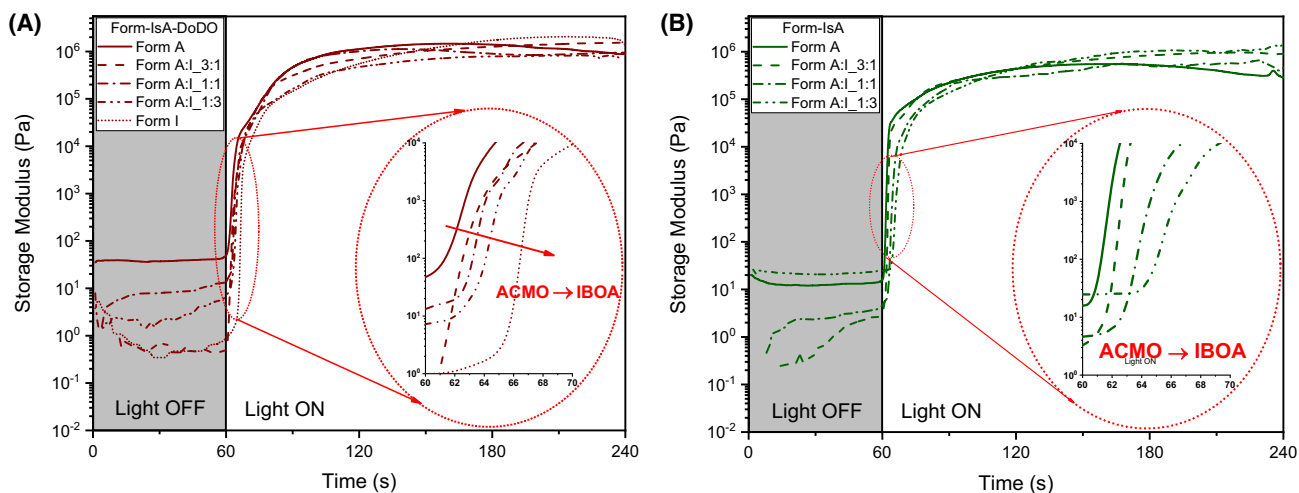
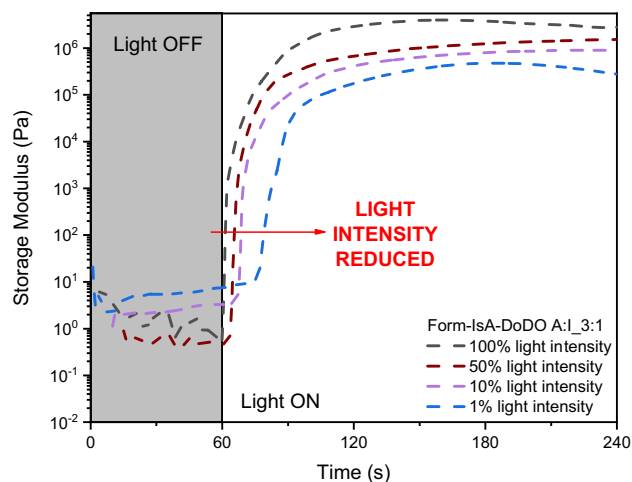


Fig. 5 Storage Modulus evolution over time for formulations (A) Form-IsA-DoDO and (B) Form-IsA

Fig. 6 Storage Modulus evolution for Form-IsA-DoDO A:I_3:1 with decreasing light intensity



rapid reaction that achieves high conversion values. Therefore, for these formulations, the requirement of a high-power light source to achieve crosslinking is eliminated. Finally, another parameter that was evaluated was the shrinkage during crosslinking. As the distance between the glass substrate and the rotating disk must be constant during the measurement, the instrument can calculate the “normal force” required to achieve it, which has been linked to shrinkage phenomena induced by radical polymerization [31]. As seen in Fig. 7, the addition of IBOA to the formulations reduced the Normal Force, which translates to a lower shrinkage. A reason for this might be the slightly slower curing, when IBOA is used, resulting in an elevated mobility of the formulation components before the vitrification point is reached.

3.4 Printed samples

After the assessment of the UV reactivity of the formulations, AM assays were performed on a DLP 3D printer. Besides typical rectangular specimen for DMA, we also attempted to print some more complex structures, given below in Fig. 8. Regardless of the diluent composition, manufacturing was accurate and precise. As a final note, the addition of IBOA lead to more flexible structures, which can be observed by the smaller and thinner pedals on the inside of

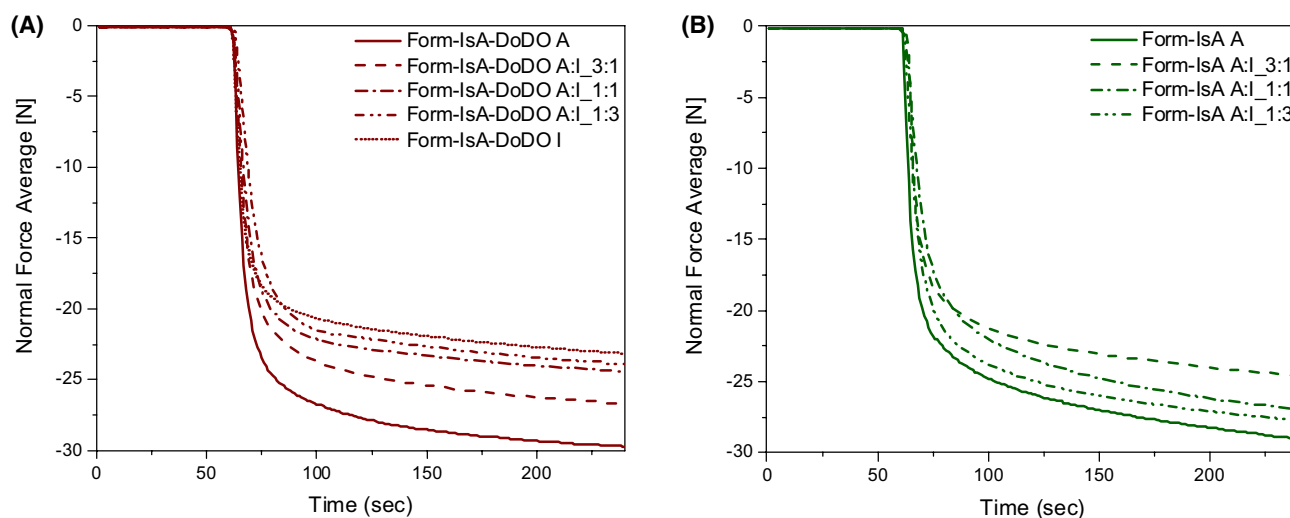


Fig. 7 Normal Force evolution of time for formulations (A) Form-IsA and (B) Form-IsA-DoDO



Fig. 8 3D-printed flower structures from formulations Form-IsA-DoDO A (left), Form-IsA-DoDO A:I 1:1 (middle) and Form-IsA-DoDO I (right)

the flower. Those appear slightly curved on the picture on the right, due to their increased flexibility compared to the ACMO based material that appears on the picture on the left.

3.5 DMA results

The thermomechanical properties of the printed materials were assessed by DMA measurements, and the results are presented in Table 4 and in Fig. 9 and Figure S3. Substitution of ACMO by IBOA at a 50% ratio resulted in formulations with lower DBD by approximately 0.5 mmol/g compared to formulations that contained only ACMO as reactive diluent. Subsequently, lower values of $\tan \delta$ and E' were observed, regardless of the polyester structure. However, it should be noted that the reduction in these mechanical properties was less pronounced in the case of the aromatic polyesters compared to the aliphatic ones. This suggests that in formulations of reduced DBD, the polyester structure is the primary parameter of influence on the mechanical properties of the crosslinked materials. This statement is also supported by the crosslinking density of the materials, calculated in Table 4. Formulations type "A" have similar values as formulations type "A:I 1:1", suggesting the density of the created network is determined by the structure of the polyester resin.

Moving to formulations from polyesters PE-IsA-50 and PE-IsA-DoDO-50, the introduction of IBOA resulted in a linear lowering of the $\tan \delta$, with the effect being more pronounced for formulations from PE-IsA-DoDO-50 that contained the long aliphatic structure of 1,12-DoDO. In that case, the glass transition temperature was lowered from 79 to 56 °C by substituting ACMO for IBOA. In the case of formulations derived from PE-IsA-50, the T_g was only 8 °C lower for the "A:I 1:3" mixture compared to the formulation that contained ACMO. This effect can be explained by the more flexible dodecanediol chains in combination with a lower double bond density of the resins. Nevertheless, this result is very

Table 4 DMA and TGA results of the printed materials presented in this study

Sample	Crosslinking density ($\cdot 10^2 \text{ mol m}^{-3}$)	Tan δ ($^\circ\text{C}$)	E'@25 $^\circ\text{C}$ (MPa)	T _{5%} ($^\circ\text{C}$)	T _{max} ($^\circ\text{C}$)	Contact angle ($^\circ$)
3D-Seb A ¹	5.6	70	270 \pm 20	275	403	– ²
3D-IsA A ¹	6.8	97	545 \pm 65	289	385	– ²
3D-SA A ¹	9.3	79	465 \pm 25	264	384	– ²
3D-PhA A ¹	6.7	90	615 \pm 5	284	377	– ²
3D-SebA A:l_1:1	5.8	59	230 \pm 10	260	407	– ²
3D-IsA A:l_1:1	6.8	94	510 \pm 30	273	398	– ²
3D-SA A:l_1:1	9.1	72	380 \pm 5	255	389	– ²
3D-PhA A:l_1:1	6.9	87	570 \pm 50	267	376	– ²
3D-IsA-DoDO A	5.7	79	361 \pm 3	285	405	67 \pm 3
3D-IsA-DoDO A:l_3:1	6.3	69	335 \pm 42	284	324/407	– ²
3D-IsA-DoDO A:l_1:1	5.9	65	288 \pm 8	291	317/409	70 \pm 4
3D-IsA-DoDO A:l_1:3	5.9	57	259 \pm 11	249	315/410	– ²
3D-IsA-DoDO I	5.6	56	268 \pm 5	279	311/412	74 \pm 5
3D-IsA A	7.6	98	422 \pm 86	291	388	68 \pm 4
3D-IsA A:l_3:1	8	96	493 \pm 95	283	312/394	– ²
3D-IsA A:l_1:1	8.1	94	507 \pm 40	277	309/405	73 \pm 3
3D-IsA A:l_1:3	8.3	92	483 \pm 76	289	311/401	79 \pm 7

¹ Results are listed from reference [15]; ² Measurement not performed

promising, as it suggests that for a given polyester structure, there is a range of temperatures within which the glass transition can be manipulated, simply by altering the ratio between the two diluents.

3.6 Contact angle

Given the difference in polarity between the two diluents that were utilized during this study and the fact that the diluent constitutes 47% of the final material, contact angle measurements were carried out to investigate whether the mixture of diluents could influence the surface properties of the crosslinked materials. Materials containing a 1:1 ACMO:IBOA ratio, and those containing only one diluent were selected, to maximize the effect on the surface properties. Results reported in Fig. 10 confirm that, though not to a great extent, there is another property of the final materials that can be altered by changing the diluent composition. A targeted selection of diluents with a more pronounced difference in hydrophobicity could lead to a more pronounced variation of the contact angle, although the reactivity and the conversion could also be influenced.

3.7 TGA

Finally, the thermal stability of the printed materials was assessed with TGA measurements. Results are shown in Fig. 11 and Figure S4 and in Table 4. Introduction of IBOA to the structure of the thermoset materials altered the thermal degradation pattern of the materials to a two-step degradation profile. The first step occurs around 300 $^\circ\text{C}$ and is attributed to the cleavage of the pendant bicyclic ester, a known degradation mechanism of this type of monomer [32]. As the content of IBOA increases, the mass loss in this temperature range is also increased. The second step is attributed to the degradation of the crosslinked section of the materials, and it takes place around 400 $^\circ\text{C}$. No relevant deviations from this degradation patterns are observed, regardless of the ACMO:IBOA composition of the materials. This suggests that the crosslinking density of these materials is the primary factor that influences their thermal stability and therefore the diluent mixture could be utilized without compromising the stability of the materials.

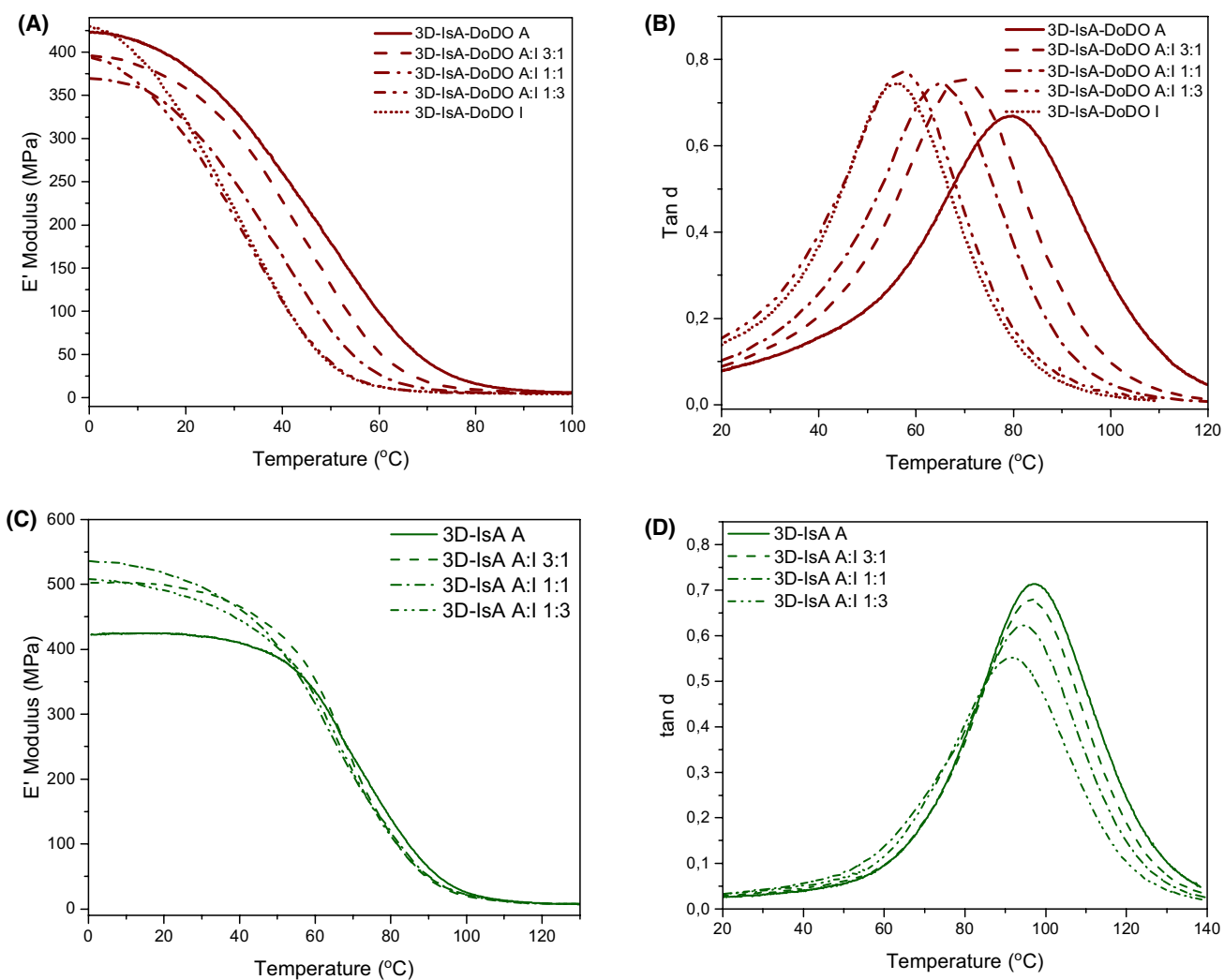


Fig. 9 DMA results of the printed materials. **(A)** E' Modulus of the materials based on PE-IsA-DoDO-50, **(B)** tan δ curves of the materials based on PE-IsA-DoDO-50, **(C)** E' Modulus of the materials based on PE-IsA-50 and **(D)** tan δ curves of the materials based on PE-IsA-50

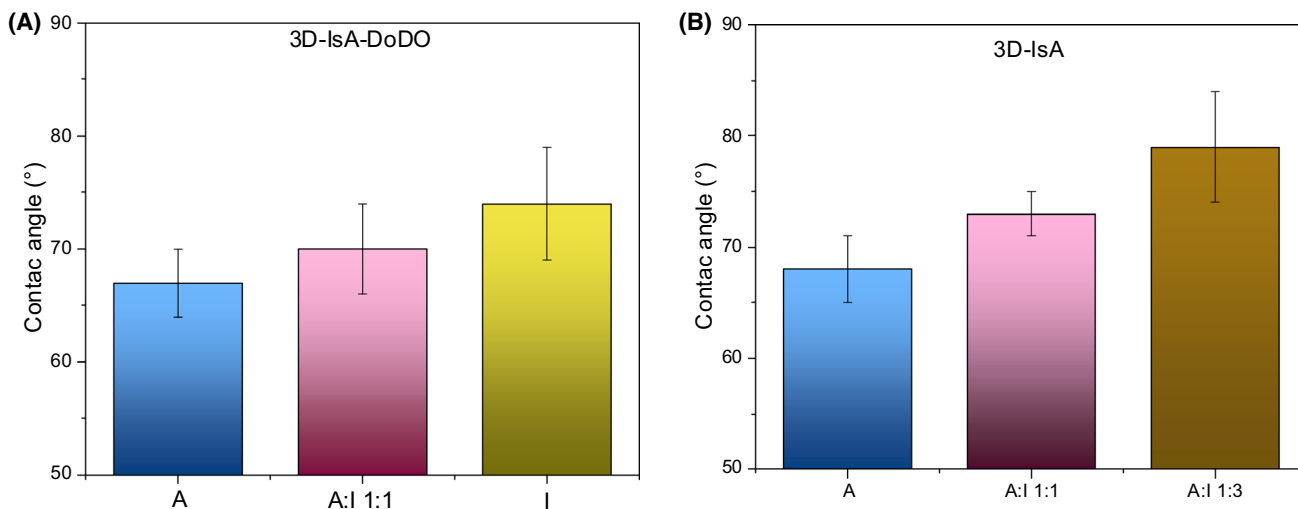


Fig. 10 Contact angle results of the printed materials based on **(A)** PE-IsA-DoDO-50 and **(B)** PE-IsA-50

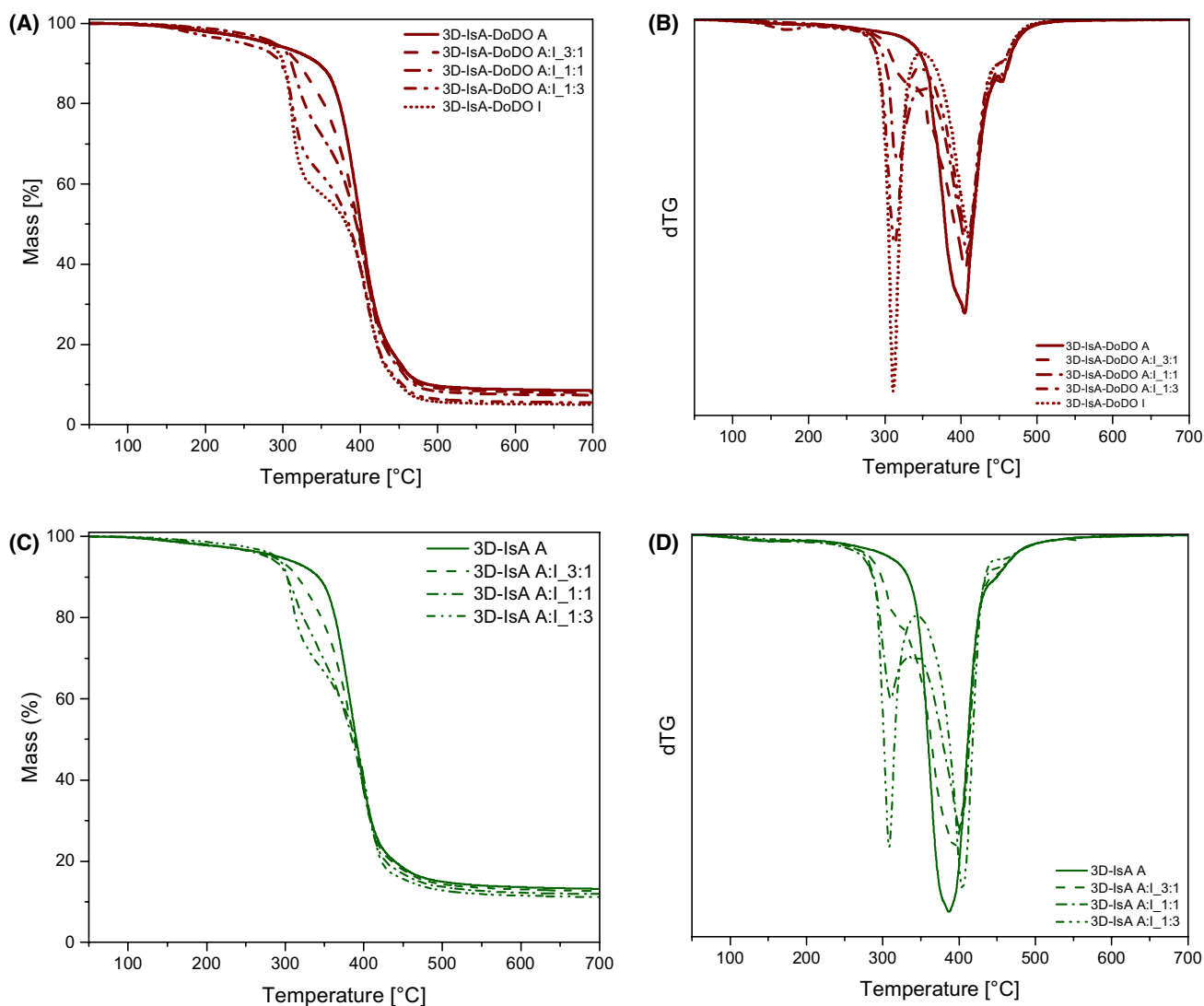


Fig. 11 Thermal stability profiles of the printed materials. **(A)** Mass loss of the materials based on PE-IsA-DoDO-50, **(B)** dTG curves of the materials based on PE-IsA-DoDO-50, **(C)** Mass loss of the materials based on PE-IsA-50 and **(D)** dTG curves of the materials based on PE-IsA-50

4 Conclusions

The main objective of the work presented herein was an in-depth structure–property study of the reactivity and performance of UV-curing AM-formulations in which the composition of the reactive diluents was modified. This objective was realized via the replacement of petrol-based ACMO with IBOA, which is a commercially available bio-based diluent. In combination with bio-based UV-curing polyester resins derived from itaconic acid, this leads to final AM-materials with high overall bio-based content. In all cases, formulations with low viscosity and adequate reactivity for UV-curing AM were obtained, while the bio-based content of the formulations was increased from 35 to more than 85%, depending on the polyester structure. It was established that the ratio between the two diluents could be used to tune reactivity related properties like the polymerization rate and the double bond conversion. Furthermore, characterization of 3D-printed specimen revealed that the thermomechanical properties of the fabricated objects could also be manipulated by altering the diluent ratio. When a polyester of flexible structure was used, a linear trend between the properties of the materials was observed. Finally, contact angle experiments showed that the surface properties of the materials could also be modified depending on the diluent content. We are therefore convinced that

these results make a significant contribution to the field of additive manufacturing, establishing the combination of diluents as viable strategy to develop materials with tunable properties. They also contribute to the enlargement of the available bio-based options for AM applications, which are limited at the moment.

Acknowledgements The research work was supported by the Hellenic Foundation for Research and Innovation (HFRI) under the 3rd Call for HFRI PhD Fellowships (Fellowship Number:6186).

This publication is based upon work from COST ActionFUR4Sustain, CA18220, supported by COST (European Cooperation in Science and Technology). The authors would like to thank Anja Gohla and Kirsten Wittenberg for their help with TGA and viscosity measurements.

Author contributions L. P. developed the synthetic plan, performed the synthesis and formulation of the materials, wrote the main manuscript text and prepared figures. L. P. performed and analyzed the insitu IR and photorheology experiments. N. M. performed the 3D-printing experiments and characterization of the printed specimen. M. S. Supervised, analyzed and evaluated the insitu IR and photorheology experiments. D. B. supervised the synthesis of the polymers, analyzed and discussed the results. T. R. conceived the experimental plan, analyzed and discussed the results of the synthesis and characterization and discussed the results, wrote main manuscript. All authors reviewed the manuscript.

Funding Open Access funding enabled and organized by Projekt DEAL. The authors have not disclosed any funding.

Data availability The data that support the findings of this study are available from the corresponding author upon reasonable request.

Declarations

Competing interests The authors declare no competing interests.

Open Access This article is licensed under a Creative Commons Attribution 4.0 International License, which permits use, sharing, adaptation, distribution and reproduction in any medium or format, as long as you give appropriate credit to the original author(s) and the source, provide a link to the Creative Commons licence, and indicate if changes were made. The images or other third party material in this article are included in the article's Creative Commons licence, unless indicated otherwise in a credit line to the material. If material is not included in the article's Creative Commons licence and your intended use is not permitted by statutory regulation or exceeds the permitted use, you will need to obtain permission directly from the copyright holder. To view a copy of this licence, visit <http://creativecommons.org/licenses/by/4.0/>.

References

1. Ligon SC, Liska R, Stampfl J, Gurr M, Mülhaupt R. Polymers for 3D printing and customized additive manufacturing. *Chem Rev*. 2017;117(15):10212–90. <https://doi.org/10.1021/acs.chemrev.7b00074>.
2. Shahbazi M, Jäger H. Current status in the utilization of biobased polymers for 3d printing process: a systematic review of the materials, processes, and challenges. *ACS Appl Bio Mater*. 2021;4(1):325–69. <https://doi.org/10.1021/acsabm.0c01379>.
3. Chyr G, DeSimone JM. Review of high-performance sustainable polymers in additive manufacturing. *Green Chem*. 2023;25(2):453–66. <https://doi.org/10.1039/D2GC03474C>.
4. Voet VS, Guit J, Loos K. Sustainable photopolymers in 3D printing: a review on biobased, biodegradable, and recyclable alternatives. *Macromol Rapid Commun*. 2021;42(3):2000475.
5. Liska R, Schuster M, Inführ R, Turecek C, Fritscher C, Seidl B, Schmidt V, Kuna L, Haase A, Varga F, Lichtenegger H, Stampfl J. Photopolymers for rapid prototyping. *J Coat Technol Res*. 2007;4(4):505–10. <https://doi.org/10.1007/s11998-007-9059-3>.
6. Pagac M, Hajnys J, Ma QP, Jancar L, Jansa J, Stefek P, Mesicek J. A review of vat photopolymerization technology: materials, applications, challenges, and future trends of 3d printing. *Polymers*. 2021;13(4):598. <https://doi.org/10.3390/polym13040598>.
7. Pezzana L, Wolff R, Melilli G, Guigo N, Sbirrazzuoli N, Stampfl J, Liska R, Sangermano M. Hot-lithography 3D printing of biobased epoxy resins. *Polym Guildf*. 2022. <https://doi.org/10.1016/j.polymer.2022.125097>.
8. Noè C, Cosola A, Tonda-Turo C, Sesana R, Delprete C, Chiappone A, Hakkarainen M, Sangermano M. DLP-Printable fully biobased soybean oil composites. *Polym Guildf*. 2022. <https://doi.org/10.1016/j.polymer.2022.124779>.
9. Yang E, Miao S, Zhong J, Zhang Z, Mills DK, Zhang LG. Bio-based polymers for 3D printing of bioscaffolds. *Polym Rev*. 2018;58(4):668–87. <https://doi.org/10.1080/15583724.2018.1484761>.
10. Guggenbiller G, Brooks S, King O, Constant E, Merckle D, Weems AC. 3D Printing of green and renewable polymeric materials: toward greener additive manufacturing. *ACS Appl Polym Mater*. 2023. <https://doi.org/10.1021/acsapm.2c02171>.
11. Maturi M, Pulignani C, Locatelli E, Vetri Buratti V, Tortorella S, Sambri L, Comes Franchini M. Phosphorescent bio-based resin for digital light processing (DLP) 3D-printing. *Green Chem*. 2020;22(18):6212–24. <https://doi.org/10.1039/d0gc01983f>.
12. Vetri Buratti V, Sanz De Leon A, Maturi M, Sambri L, Molina SI, Comes Franchini M. Itaconic-acid-based sustainable poly (ester amide) resin for stereolithography. *Macromolecules*. 2022;55(8):3087–95. <https://doi.org/10.1021/acs.macromol.1c02525>.
13. Pérocheau Arnaud S, Andreou E, Pereira Köster LVG, Robert T. Selective synthesis of monoesters of itaconic acid with broad substrate scope: biobased alternatives to acrylic acid? *ACS Sustain Chem Eng*. 2020;8(3):1583–90. <https://doi.org/10.1021/acssuschemeng.9b06330>.

14. Pérocheau Arnaud S, Malitowski NM, Meza Casamayor K, Robert T. Itaconic acid-based reactive diluents for renewable and acrylate-free UV-curing additive manufacturing materials. *ACS Sustain Chem Eng.* 2021;9(50):17142–51. <https://doi.org/10.1021/acssuschemeng.1c06713>.
15. Papadopoulos L, Malitowski NM, Bikiaris D, Robert T. Bio-based additive manufacturing materials: an in-depth structure-property relationship study of UV-curing polyesters from itaconic acid. *Eur Polym J.* 2023;186: 111872. <https://doi.org/10.1016/j.eurpolymj.2023.111872>.
16. Weng Z, Huang X, Peng S, Zheng L, Wu L. 3D Printing of ultra-high viscosity resin by a linear scan-based vat photopolymerization system. *Nat Commun.* 2023;14(1):4303. <https://doi.org/10.1038/s41467-023-39913-4>.
17. Zhang J, Xiao P. 3D Printing of photopolymers. *Polym Chem.* 2018;9(13):1530–40. <https://doi.org/10.1039/C8PY00157J>.
18. Mehta LB, Wadgaonkar KK, Jagtap RN. Synthesis and characterization of high bio-based content unsaturated polyester resin for wood coating from itaconic acid: effect of various reactive diluents as an alternative to styrene. *J Dispers Sci Technol.* 2019;40(5):756–65. <https://doi.org/10.1080/01932691.2018.1480964>.
19. *European Commission Directive 1999/45 of 31 May (1999).*
20. *Classification and labelling changes of N-vinyl caprolactam.* <https://esma.com/51-news-sp-665/newsflashes/556-esma-information-note-new-classification-and-labelling-for-n-vinyl-caprolactam> (accessed 2023–03–21).
21. Vihola H, Laukkanen A, Valtola L, Tenhu H, Hirvonen J. Cytotoxicity of thermosensitive polymers poly(N-isopropylacrylamide), poly(N-vinylcaprolactam) and amphiphilically modified poly(N-vinylcaprolactam). *Biomaterials.* 2005;26(16):3055–64. <https://doi.org/10.1016/j.biomaterials.2004.09.008>.
22. Su Y, Zhang S, Zhou X, Yang Z, Yuan T. A novel multi-functional bio-based reactive diluent derived from cardanol for high bio-content UV-curable coatings application. *Prog Org Coat.* 2020. <https://doi.org/10.1016/j.porgcoat.2020.105880>.
23. Wei G, Xu H, Chen L, Li Z, Liu R. Isosorbide-based high performance UV-curable reactive diluents. *Prog Org Coat.* 2019;126:162–7. <https://doi.org/10.1016/j.porgcoat.2018.10.028>.
24. Liu J, Wang S, Peng Y, Zhu J, Zhao W, Liu X. Advances in sustainable thermosetting resins: from renewable feedstock to high performance and recyclability. *Prog Polym Sci.* 2021;113: 101353. <https://doi.org/10.1016/j.progpolymsci.2020.101353>.
25. Papadopoulos L, Pezzana L, Malitowski NM, Sangermano M, Bikiaris DN, Robert T. UV-Curing additive manufacturing of bio-based thermosets: effect of diluent concentration on printing and material properties of itaconic acid-based materials. *ACS Omega.* 2023;8(34):31009–20. <https://doi.org/10.1021/acsomega.3c02808>.
26. Prandato E, Livi S, Melas M, Auclair J, Verney V, Fleury E, Méchin F. Effect of bio-based monomers on the scratch resistance of acrylate photopolymerizable coatings. *J Polym Sci B Polym Phys.* 2015;53(5):379–88. <https://doi.org/10.1002/polb.23641>.
27. Murayama T, Bell JP. Relation between the network structure and dynamic mechanical properties of a typical amine-cured epoxy polymer. *J Polym Sci Part A2 Polym Phys.* 1970;8(3):437–45.
28. US3951934A: Polymerization of Acrylamide in the Presence of Water-Soluble Compounds. <https://patents.google.com/patent/US3951934A/en> (accessed 2024–02–20).
29. Xiang N, Li C, Yang K, Yang C, Guo H, Wang C. Energy saving technology of acrylamide polymerization in plate reactor based on phase change heat transfer. *Appl Therm Eng.* 2023;227: 120358. <https://doi.org/10.1016/j.applthermaleng.2023.120358>.
30. Dainton FS, Ivin KJ, Walmsley DAG. The heats of polymerization of some cyclic and ethylenic compounds. *Trans Faraday Soc.* 1960;56:1784. <https://doi.org/10.1039/tf9605601784>.
31. Gorsche C, HariKrishna R, Baudis S, Knaack P, Husar B, Laeuger J, Hoffmann H, Liska R. Real time-NIR/MIR-photorheology: a versatile tool for the in situ characterization of photopolymerization reactions. *Anal Chem.* 2017;89(9):4958–68. <https://doi.org/10.1021/acs.analchem.7b00272>.
32. Ors JA, la Perriere DM. Thermogravimetric profile of decomposition of acrylate systems based on bornyl acrylate monomers. *Polym Guildf.* 1986;27(12):1999–2002. [https://doi.org/10.1016/0032-3861\(86\)90197-7](https://doi.org/10.1016/0032-3861(86)90197-7).

Publisher's Note Springer Nature remains neutral with regard to jurisdictional claims in published maps and institutional affiliations.